Open Access Series of Imaging Studies (OASIS): Cross-sectional MRI Data in Young, Middle Aged, Nondemented, and Demented Older Adults

Daniel S. Marcus[1], Tracy H. Wang[1], Jamie Parker[2], John G. Csernansky[1], John C. Morris[1], and Randy L. Buckner[2,3,4]

Abstract

■ The Open Access Series of Imaging Studies is a series of magnetic resonance imaging data sets that is publicly available for study and analysis. The initial data set consists of a cross-sectional collection of 416 subjects aged 18 to 96 years. One hundred of the included subjects older than 60 years have been clinically diagnosed with very mild to moderate Alzheimer's disease. The subjects are all right-handed and include both men and women. For each subject, three or four individual T1-weighted magnetic resonance imaging scans obtained in single imaging sessions are included. Multiple within-session acquisitions provide extremely high contrast-to-noise ratio, making the data amenable to a wide range of analytic approaches including automated computational analysis. Additionally, a reliability data set is included containing 20 subjects without dementia imaged on a subsequent visit within 90 days of their initial session. Automated calculation of whole-brain volume and estimated total intracranial volume are presented to demonstrate use of the data for measuring differences associated with normal aging and Alzheimer's disease. ■

INTRODUCTION

The Open Access Series of Imaging Studies (OASIS) is a project aimed at making magnetic resonance imaging (MRI) data sets of the brain freely available to the scientific community. By compiling and freely distributing MRI data sets, we hope to facilitate future discoveries in basic and clinical neuroscience. Specifically, the OASIS project is intended to play a number of roles. First, OASIS images and related measures serve as data sets for continued scientific exploration. Beginning with the initial set of images obtained from more than 400 individuals with and without dementia across the adult life span, OASIS data sets are selected to encourage investigation of high interest topics and provide data that would be difficult for individual laboratories to acquire. Second, OASIS data are targets for researchers creating and furthering analytic techniques. Because the images are acquired from subjects over a range of ages and health conditions, OASIS data can be used to test the robustness and validity of techniques across the full range of the human brain's varied landscapes. Third, OASIS data can be used as benchmark targets for comparing similar analytic techniques. Standard images provide a common point of reference for demonstrating and contrasting methods. By providing carefully screened

data in an open-access fashion, the OASIS project can provide such exemplar images to the neuroimaging community. Finally, OASIS data can be used for educational purposes as examples or as working data sets for courses and workshops.

A number of data-sharing procedures have been adopted by the OASIS project to ensure the integrity and usability of the provided data.

1. Quality control. All images are carefully screened for acquisition and processing errors. Images with severe artifacts are excluded from the distribution. Images with visible artifacts typical of MR acquisitions are included. This variability in quality is intended to provide tool builders with realistic target images.

2. Documentation. Detailed acquisition protocols and parameters, demographics, and supporting measures (e.g., Mini-Mental State Examination [MMSE] scores) are provided for all included images.

3. Preparation. In addition to the raw acquisition data, images representing common postprocessing procedures (e.g., atlas registration, bias field correction) are distributed as a convenience and for comparison with similar postprocessing methods.

4. Anonymization. In compliance with privacy regulations, distributed data are assigned random identification numbers (IDs), and all identifying information are removed from the image files. All links between original and random IDs are permanently destroyed before release.

[1]Washington University, [2]Harvard University, [3]Massachusetts General Hospital, [4]Howard Hughes Medical Institute

5. Access. The data are available on DVD and accessible for viewing and downloading via a dedicated Web site. Third parties are encouraged to redistribute the data in ways that add to its general availability.

6. Ongoing support. The OASIS Web site will serve as a forum for announcements and discussions regarding the distributions and as a clearinghouse for third party derived data sets.

7. Unrestricted usage. OASIS data may be freely used with no restrictions. Attributions to the OASIS project will lend to the credence of OASIS as a reference resource. Anyone wishing to distribute derived data will be encouraged to include the original images. The OASIS Data Use Agreement is available at www.oasis-brains.org.

In the remainder of this article, we describe the first OASIS data set release. This release includes cross-sectional data from 416 individuals across the adult life span age 18 to 96 years, including 100 individuals with very mild to moderate Alzheimer's disease (AD) as diagnosed clinically and characterized using the Clinical Dementia Rating (CDR) scale (Morris et al., 2001; Morris, 1993). Cross-sectional data have proven useful in studying normal and diseased aging for both global (whole-brain) and local structure. In normal aging, whole-brain volume decline begins in early adulthood and accelerates in advanced aging (DeCarli et al., 2005; Fotenos, Snyder, Girton, Morris, & Buckner, 2005; Sowell, Thompson, Leonard, et al., 2004; Durston, 2003; Blatter et al., 1995). Preferential volume loss of gray matter (Raz, Williamson, Gunning-Dixon, Head, & Acker, 2000) and regionally specific thinning of the cortex are also noted (Salat et al., 2004). Level of education, sex, socioeconomic status, and cardiovascular health have been identified as contributing factors in volume decline in advanced aging, suggesting that subclinical health conditions contribute to age-related changes in brain structure (Fotenos, Mintun, Snyder, Morris, & Buckner, in press; Raz, Rodrigue, & Acker, 2003; Koga et al., 2002; Coffey, Saxton, Ratcliff, Bryan, & Lucke, 1999; Coffey et al., 1998). Individuals with clinically diagnosed AD show substantially reduced overall brain volumes relative to age-matched peers as well as regional volume loss that has been well documented in the hippocampal formation, among other regions (e.g., Jack et al., 1997; Raz et al., 1997; Killiany et al., 1993; Jack, Petersen, O'Brien, & Tangalos, 1992; Scheltens et al., 1992). Cross-sectional MRI data have also been used to facilitate and validate analytic tools and algorithms, including atlas-based head size normalization (Buckner et al., 2004), automated whole-brain segmentation (Fischl et al., 2002), automated labeling of cerebral cortex into regions of interest (Desikan et al., 2006), and large-deformation maps of brain structure shape (Csernansky, Wang, Joshi, Ratnanather, & Miller, 2004).

METHODS

Subjects

Subjects aged 18 to 96 years were selected from a larger database of individuals who had participated in MRI studies at Washington University, based on the availability of at least three acquired T1-weighted images, right-hand dominance, and a recent clinical evaluation for older adults. Young and middle-aged subjects were recruited from the Washington University community. Older subjects with and without dementia were obtained from the longitudinal pool of the Washington University Alzheimer Disease Research Center (ADRC). The ADRC's normal and cognitively impaired subjects were recruited primarily through media appeals and word of mouth, with 80% of subjects initiating contact with the center and the remainder being referred by physicians (Berg et al., 1982, 1998). All subjects participated in accordance with guidelines of the Washington University Human Studies Committee. Approval for public sharing of the data was also specifically obtained.

All subjects were screened for inclusion in this release. Young and middle-aged adults were questioned before image acquisition by a trained technician about their medical histories and use of psychoactive drugs. Older adults, aged 60 and older, underwent the ADRC's full clinical assessment as described below. Subjects with a primary cause of dementia other than AD (e.g., vascular dementia, primary progressive aphasia), active neurological or psychiatric illness (e.g., major depression), serious head injury, history of clinically meaningful stroke, and use of psychoactive drugs were excluded, as were subjects with gross anatomical abnormalities evident in their MRI images (e.g., large lesions, tumors). However, subjects with age-typical brain changes (e.g., mild atrophy, leukoaraiosis) were accepted. MRI acquisitions typically were obtained within a year of a subject's clinical assessment (mean = 105 days, range = 0–314 days). Three subjects with AD were scanned after a somewhat longer duration (635, 449, and 443 days). The final data set includes 416 subjects. Twenty subjects in their twenties were imaged on a second occasion within 90 days of their initial session to provide a means for assessing reliability of data acquisition and analysis.

Portions of the clinical, demographic, and image data obtained from subjects in this release have been used in previous studies (Buckner et al., 2004, 2005, in press; Burns et al., 2005; Fotenos et al., 2005, in press; Head, Snyder, Girton, Morris, & Buckner, 2005; Salat et al., 2004) and made publicly available, using different anonymous identifiers, via the fMRI Data Center under accession number 2-2004-1168x.

Clinical Assessment

Dementia status was established and staged using the CDR scale (Morris et al., 2001; Morris, 1993). The deter-

mination of AD or control status is based solely on clinical methods, without reference to psychometric performance, and any potential alternative causes of dementia (known neurological, medical, or psychiatric disorders) must be absent. The diagnosis of AD is based on clinical information (derived primarily from a collateral source) that the subject has experienced gradual onset and progression of decline in memory and other cognitive and functional domains. Specifically, the CDR is a dementia-staging instrument that rates subjects for impairment in each of the six domains: memory, orientation, judgment and problem solving, function in community affairs, home and hobbies, and personal care. Based on the collateral source and subject interview, a global CDR score is derived from individual ratings in each domain. A global CDR of 0 indicates no dementia, and CDRs of 0.5, 1, 2, and 3 represent very mild, mild, moderate, and severe dementia, respectively. These methods allow for the clinical diagnosis of AD in individuals with a CDR of 0.5 or greater, based on standard criteria (McKhann et al., 1984), that is confirmed by histopathological examination in 93% of the individuals (Berg et al., 1998), even for those in the earliest symptomatic stage (CDR 0.5) of AD who elsewhere may be considered to represent ''mild cognitive impairment'' (Storandt, Grant, Miller, & Morris, 2006).

Image Acquisition

For each subject, 3–4 individual T1-weighted magnetization prepared rapid gradient-echo (MP-RAGE) im-

Table 1. MRI Acquisition Details

Sequence	MP-RAGE
TR (msec)	9.7
TE (msec)	4.0
Flip angle (°)	10
TI (msec)	20
TD (msec)	200
Orientation	Sagittal
Thickness, gap (mm)	1.25, 0
Slice number	128
Resolution (pixels)	256 × 256 (1 × 1 mm)

ages (Mugler & Brookeman, 1990) were acquired on a 1.5-T Vision scanner (Siemens, Erlangen, Germany) in a single imaging session. Head movement was minimized by cushioning and a thermoplastic face mask. Headphones were provided for communication. A vitamin E capsule was placed over the left forehead to provide a reference marker of anatomical side. Positioning was low in the head coil (toward the feet) to optimize imaging of the cerebral cortex. MP-RAGE parameters were empirically optimized for gray–white contrast (Table 1). An example of typical images is illustrated in Figure 1.
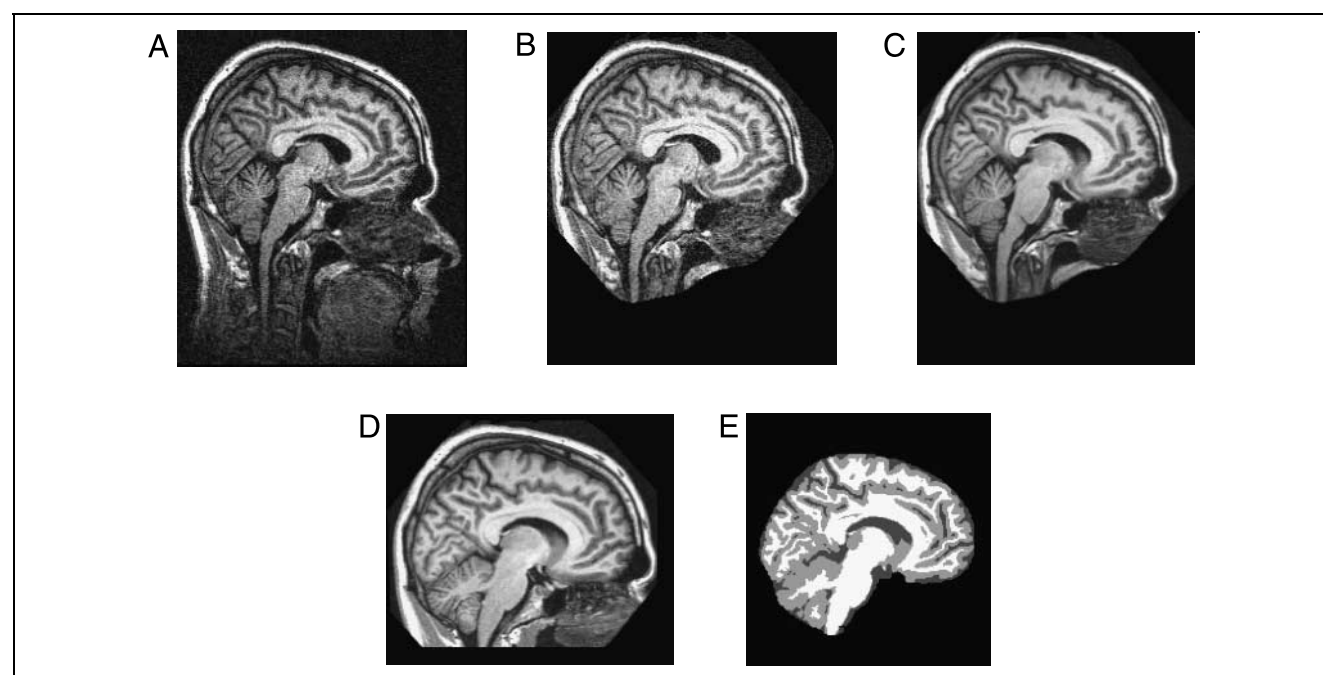

Figure 1. Typical MRI data set. (A) Individual scan before defacing. (B) Same scan after defacing. Note that the defacing process leaves the cranial vault intact while identifying facial features are removed. (C) Averaged motion-corrected image. Note improved signal-to-noise ratio. (D) Atlas-registered gain-field-corrected image. (E) Tissue classification image.

Postprocessing

For each subject, the individual scan files were converted from Siemens proprietary IMA format into 16-bit Analyze 7.5 format using a custom conversion program. Sensitive header fields (patient ID, experiment date) were left blank. Identifying facial features were then removed from the images using software provided by the fMRI Data Center (www.fmridc.org). This method first masks out all nonbrain voxels in the image, dilates and smoothes the mask in an iterative fashion, and finally applies the enlarged mask to the original image to safely remove voxels outside the cranial vault. In 12 cases where this method either left too much of the face present or invasively cut into the cranial vault, de-identification was done using software provided by the Morphometry Biomedical Informatics Research Network (www.nbirn.net). This method registers the image to an atlas in which facial features and brain tissue have been hand-labeled. All voxels in the image that have a zero probability of being brain and a nonzero probability of being face are assigned an intensity value of zero. The de-identified images are the images included in the present distribution and were used in all subsequent processing and analyses described here.

The images were then corrected for interscan head movement and spatially warped into the atlas space of Talairach and Tournoux (1988) using a rigid transformation that differs in process from the original piecewise scaling. The resulting transformation nonetheless places the brains in the same coordinate system and bounding box as the original atlas. The template atlas used here consisted of a combined young-and-old target previously generated from a representative sample of young subjects ($n = 12$) and old subjects without dementia ($n = 12$). The use of a combined template has been shown to minimize the potential bias of an atlas normalization procedure to overexpand atrophied brains (Buckner et al., 2004). For registration, a 12-parameter affine transformation was computed to minimize the variance between the first MP-RAGE image and the atlas target (Snyder, 1996). The remaining MP-RAGE images were registered to the first (in-plane stretch allowed) and resampled via transform composition into a 1-mm isotropic image in atlas space. The result was a single, high-contrast, averaged MP-RAGE image in atlas space. Subsequent steps included skull removal by application of a loose-fitting atlas mask and correction for intensity inhomogeneity due to non-uniformity in the magnetic field. Intensity variation was corrected across contiguous regions, based on a quadratic inhomogeneity model fitted to data from a phantom (Styner, Brechbuhler, Szekely, & Gerig, 2000).

Estimated Total Intracranial Volume and Normalized Whole-brain Volume

The procedures used for measuring intracranial and whole-brain volumes have been described in detail previously (Fotenos et al., 2005; Buckner et al., 2004). In brief, estimated total intracranial volume (eTIV) was computed by scaling the manually measured intracranial volume of the atlas by the determinant of the affine transform connecting each individual to the atlas. This method has been shown to be proportional to manually measured total intracranial volume (TIV, $r = 0.94$) and minimally biased by atrophy (Buckner et al., 2004).

Normalized whole-brain volume (nWBV) was computed using the FAST program in the FSL software suite (www.fmrib.ox.ac.uk/fsl) (Zhang, Brady, & Smith, 2001). The image was first segmented to classify brain tissue as cerebral spinal fluid, gray matter, or white matter. The segmentation procedure iteratively assigned voxels to tissue classes based on maximum likelihood estimates of a hidden Markov random field model. The model used spatial proximity to constrain the probability with which voxels of a given intensity are assigned to each tissue class. Finally, nWBV was computed as the proportion of all voxels within the brain mask classified as gray or white matter. The unit of normalized volume is percent, which represents the percentage of the total segmented voxels within the eTIV (Fotenos et al., 2005).

Quality Control

All images in the set were carefully screened for artifacts, acquisition problems, and processing errors. During the screening process, each image was viewed on a per-slice basis along each principal axis. Each image was assigned a value from 1 to 3, with 1 indicating a high-quality image, 2 indicating a scan with minor flaws, and 3 indicating severe flaws. Typical flaws included electronic noise resulting in bright lines through multiple slices, motion artifacts appearing as hazy bands across the image, poor head positioning resulting in wraparound artifacts, distortions from dental work, and limited image contrast (Figure 2). Images with a rating of 3 were excluded from the data set. A number of borderline images remain in the distribution, providing tool builders and testers with a realistic range of acquisition quality. In cases where individual scans were deemed unusable, the single scan was removed from the set but the remainder of the subject's scans was included. Overall, 10 individual scans and 15 complete sessions were excluded from the final release due to poor image quality.

RESULTS

Overview of the Data Set

The current data set consists of subjects across the adult life span (Table 2). It includes 218 subjects aged 18 to 59 years and 198 subjects aged 60 to 96 years. The overall age distribution is presented in Figure 3. Each group includes an approximately equal number of male and female subjects. Of the older subjects, 98 had a CDR
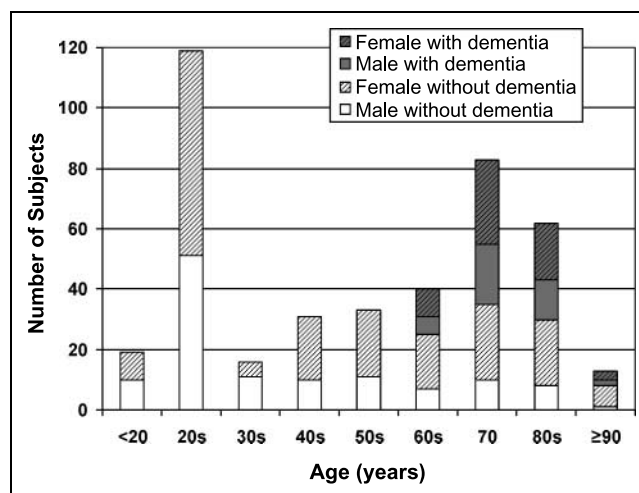
Figure 2. Example images illustrate the quality control rating procedures. (A) A scan that received a rating of 1, indicating a high-quality image with minimal artifacts and high contrast. (B) A scan that received a rating of 3 because significant motion artifacts. Such artifacts are particularly apparent when scrolling through multiple image slices. (C) A scan that received a rating of 2 because of significant in-plane wraparound. Because the nose does not actually overlap into brain tissue, this scan was retained in the data set. Such borderline images were relatively rare. (D) A scan that received a rating of 3 because of severe in-plane wraparound that cuts into the brain.

score of 0, indicating no dementia, and 100 had a CDR score greater than zero (70 CDR = 0.5, 28 CDR = 1, 2 CDR = 2), indicating a diagnosis of very mild to moderate AD. Additional demographics and clinical characteristics of the older subjects are shown in Table 3.

Anatomical Characteristics

As a means of determining whether defacing techniques impact morphometric analysis, eTIV and nWBV were calculated before and after defacing for each subject.

The slope of the best fit line was 1.00 (r = 1.00) for eTIV and was 1.00 (r = 1.00) for nWBV. The mean absolute percent differences before and after defacing were 0.024% for eTIV and 0.059% for nWBV. The defacing process, therefore, has little impact on morphometric measures of interest.

Having established that defacing has minimal impact, eTIV and nWBV are plotted across the adult life span in Figure 4 for the data included as part of the OASIS distribution. Analyses are selective and used to illustrate properties of the data. More detailed normative estimates of

Table 2. Age and Diagnosis Characteristics of the Data Set

Age Group	Total n	Without Dementia				With Dementia				CDR 0.5/1/2
		n	Mean	Male	Female	n	Mean	Male	Female	
<20	19	19	18.53	10	9	0		0	0	0/0/0
20s	119	119	22.82	51	68	0		0	0	0/0/0
30s	16	16	33.38	11	5	0		0	0	0/0/0
40s	31	31	45.58	10	21	0		0	0	0/0/0
50s	33	33	54.36	11	22	0		0	0	0/0/0
60s	40	25	64.88	7	18	15	66.13	6	9	12/3/0
70s	83	35	73.37	10	25	48	74.42	20	28	32/15/1
80s	62	30	84.07	8	22	32	82.88	13	19	22/9/1
≥90	13	8	91.00	1	7	5	92.00	2	3	4/1/0
Total	416	316		119	197	100		41	59	

Figure 3. Subjects by age, sex, and dementia status. Because of the recruiting requirements of studies included in the database from which the data set was culled, a disproportionately large number of younger subjects were available. Nonetheless, at least 15 subjects are included in each decade, allowing for continuous sampling of the adult life span.

eTIV and nWBV can be found in the study of Fotenos et al. (2005) and Buckner et al. (2004). In the present sample, eTIV showed a trend for a small age effect [$R^2 = 0.0022$, $F(1,158) = 0.35$, $p = .06$ in men, and $R^2 = 0.12$, $F(1,254) = 2.98$, $p = .09$ in women] and a strong sex effect in each of the young, middle-aged, old without dementia, and old with dementia groups [$t(215) = 10.81$, $t(95) = 6.42$, $t(97) = 5.41$, respectively; all $p < .001$]. Consistent with our prior work (Buckner et al., 2005), direct eTIV comparison of age-matched groups with and without de-
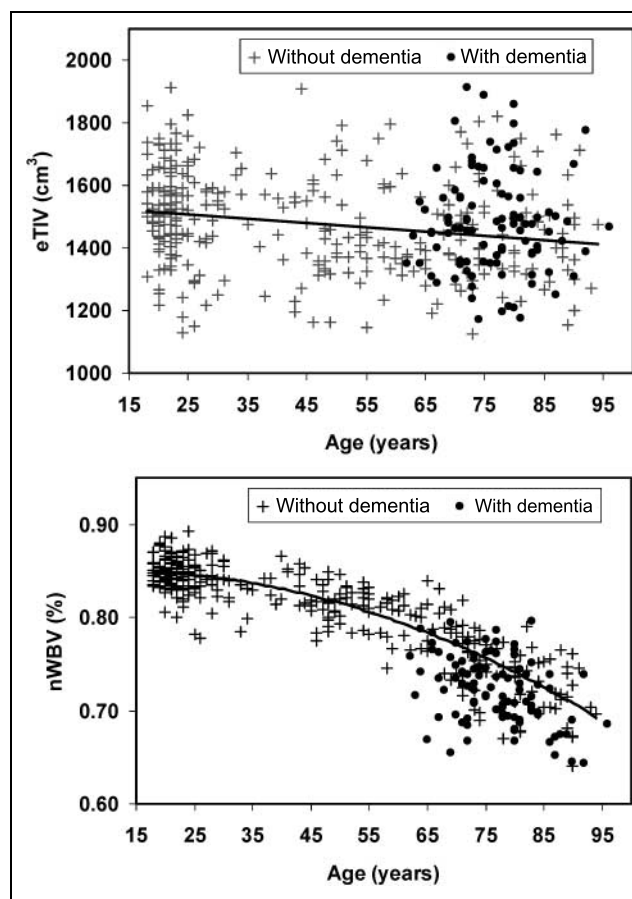
Figure 4. Plots of automated anatomical measures by age. Each point represents a unique subject from a single scanning session. (Top) eTIV: The best-fit line is drawn for individuals without dementia only. (Bottom) nWBV: The best-fit polynomial regression is drawn for individuals without dementia only.

Table 3. Sample Characteristics of Older Subjects

	CDR = 0	CDR = 0.5	CDR = 1	CDR = 2
Number	98	70	28	2
Sex (female/male)	72/26	39/31	19/9	1/1
Age (years)	75.9 ± 9.0 (60–94)	76.4 ± 7.0 (63–92)	77.2 ± 7.5 (62–96)	82 ± 5.7 (78–86)
Education (years)	14.5 ± 2.9 (8–23)	13.8 ± 3.2 (6–20)	12.9 ± 3.2 (7–20)	11 ± 4.2 (8–14)
MMSE score	29.0 ± 1.2 (25–30)	25.6 ± 3.5 (14–30)	21.7 ± 3.8 (15–29)	15.0 ± 0.0 (15)
Prescriptions (n)	2.8 ± 2.1 (0–8)	2.5 ± 2.0 (0–8)	2.2 ± 2.0 (0–6)	1.5 ± 0.7 (1–2)
Systolic BP (mmHg)	134.2 ± 19.2 (100–192)	142.6 ± 20.2 (104–188)	146.0 ± 25.6 (90–192)	148.0 ± 11.3 (140–156)
Diastolic BP (mmHg)	71.9 ± 10.3 (40–96)	72.7 ± 9.4 (59–90)	74.5 ± 10.6 (60–96)	88.0 ± 19.8 (74–102)
Reported HBP (%)	42.7	43.2	46.4	50.0
Diabetes (%)	9.1	11.6	17.2	0.0

The sample consisted of 198 individuals (98 without dementia and 100 with AD). Values given are mean ± *SD*. Values in parentheses represent the range. Full clinical data were not available for 23 subjects. Compared with the adults without dementia, the older adults with dementia had lower scores on the MMSE [$t(194) = 10.66$, $p < .001$] and slightly fewer years of education [$t(194) = 2.60$, $p < .05$].

MMSE scores range from 30 (*best*) to 0 (*worst*).

HBP = high blood pressure.

mentia failed to reach significance for either the men [$t(76) = 0.08, p = .94$] or women [$t(153) = 1.18, p = .24$].

Consistent with the literature, nWBV showed a significant decrease in individuals without dementia across the adult life span (18–95 years) [$R^2 = 0.75, F(2,313) = 485.7, p < .001$]. Adding a quadratic term improved the fit of the model [$R^2 = 0.78, F(2,313) = 557.1, p < .001$]. The decrease in nWBV with age was significant even in the 18- to 30-year-old group [$R^2 = 0.048, F(2,138) = 3.9, p < .05$]. Taken together, these results show brain volume loss begins early in life and accelerates in advanced aging. Individuals with AD exhibited marked nWBV reduction disproportionate to age. Analysis of variance with age, sex, and dementia status as covariates was significant [$R^2 = 0.44, F(194,3) = 50.4, p < .001$], with main effects for age and dementia status ($p < .001$) and a trend for an effect of sex ($p = .06$).

Reliability Scans

To provide a benchmark for determining the reliability of analytic procedures, 20 subjects were scanned on two separate occasions with a mean delay of 20.55 days (range = 1–89 days). These subjects did not have dementia and ranged in age from 19 to 29 years. Because of the short latency between scan sessions, differences in the images and measures derived from them are unlikely to be attributable to anatomical change and instead can be attributed to sources of noise (e.g., head positioning, day-to-day scanner variability) and instability in analytic procedures. Figure 5 shows eTIV (top) and nWBV (bottom) from the first session versus the second session for each subject in the reliability data set. The mean absolute percent difference was 0.54% for eTIV and 0.44% for nWBV. The coefficients of variation (CVs, the standard deviation of the difference between test and retest volumes divided by the overall mean, expressed in percent) were 0.47% for eTIV and 0.44% for nWBV.

Obtaining and Using the Data

OASIS data can be obtained at www.oasis-brains.org. Requests for DVD distributions of the data can be submitted at the Web site. For convenience, we also provide the data using the open-source Extensible Neuroimaging Archive Toolkit (Marcus, Olsen, Ramaratnam, & Buckner, 2007). It provides tools to search, visualize, and download the data. Before downloading and requesting data, users are asked to abide by the OASIS Data Usage Agreement.

OASIS data are distributed in GNU zip archive files, which can be uncompressed using freely available software. All images are distributed in Analyze 7.5 format, which can be visualized and processed using a number of commercial and open source applications, including Neurolens, ImageJ, and MRIcro. For each imaging ses-
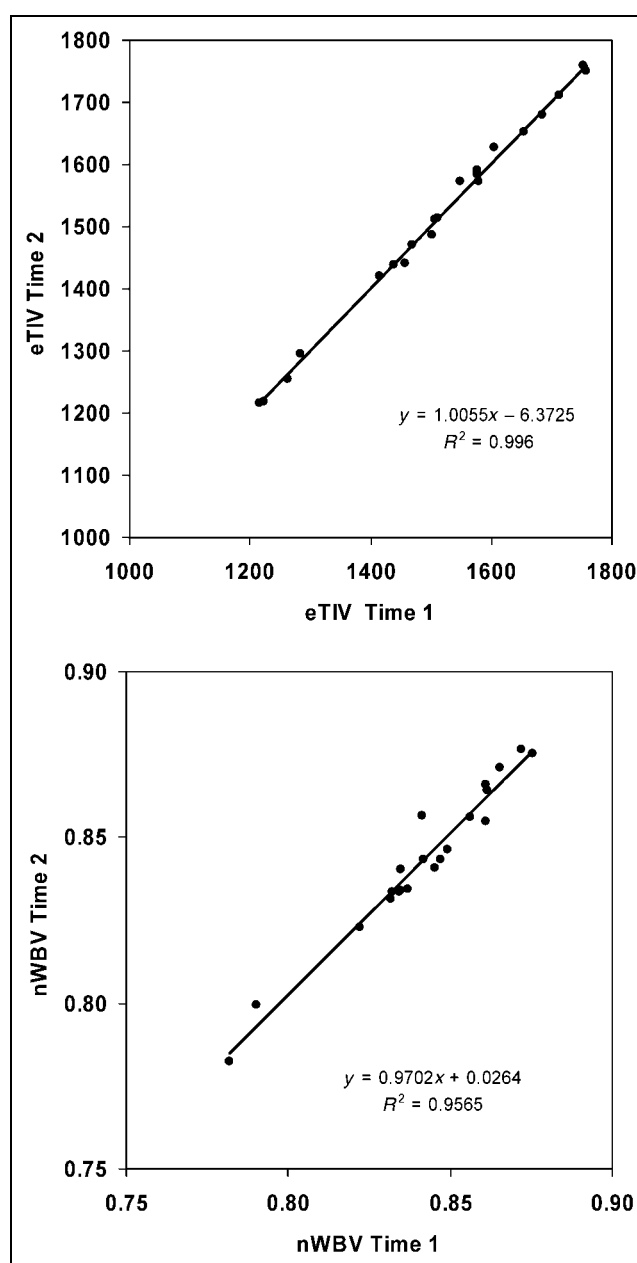

Figure 5. Plots of automated anatomical measures for reliability scans. Each point represents the values of the anatomical measure calculated from images obtained from the same subject without dementia on two separate scan sessions separated by a short interval (<90 days). The reliability of eTIV (top, $r = 0.99$) and nWBV (bottom, $r = 0.96$) are high.

sion, the following image files are included in the distribution: three to four individual scan images; an image in which the individual scans have been aligned and coregistered; an image that has been gain-field-corrected and registered to the atlas of Talairach and Tournoux (1988) (henceforth T88); a masked T88 image in which the intensity of all nonbrain voxels has been set to zero; and a segmented T88 image in which each voxel has been labeled as gray matter, white matter, or cerebral spinal fluid. Demographic, clinical, and derived

Table 4. Measures Included in the Data Set

Age	Age at time of image acquisition (years)
Sex	Sex (male or female)
Education	Years of education
Socioeconomic status	Assessed by the Hollingshead Index of Social Position and classified into categories from 1 (*highest status*) to 5 (*lowest status*) (Hollingshead, 1957)
MMSE score	Ranges from 0 (*worst*) to 30 (*best*) (Folstein, Folstein, & McHugh, 1975)
CDR scale	0 = no dementia, 0.5 = very mild AD, 1 = mild AD, 2 = moderate AD (Morris, 1993)
Atlas scaling factor	Computed scaling factor (unitless) that transforms native-space brain and skull to the atlas target (i.e., the determinant of the transform matrix) (Buckner et al., 2004)
eTIV	Estimated total intracranial volume (cm^3) (Buckner et al., 2004)
nWBV	Expressed as the percent of all voxels in the atlas-masked image that are labeled as gray or white matter by the automated tissue segmentation process (Fotenos et al., 2005)

imaging measures (Table 4) are available in XML and spreadsheet formats. Additional details of the directory structure, file naming scheme, and image characteristics can be found at www.oasis-brains.org/pdf/oasis_cross-sectional_facts.pdf.

DISCUSSION

The present data set includes T1-weighted MRI data from 416 individuals aged 18 to 96 years, including 100 individuals clinically diagnosed with AD. Multiple acquisitions are included for each subject, allowing extremely high contrast properties after image averaging. These data are amenable to a range of analysis procedures. The data have been de-identified, carefully screened for image quality, and postprocessed to generate common anatomical measures. These data are available under a liberal usage policy that allows free access to all interested parties.

To accommodate public release of the data, the original images were processed to remove facial features. The methods used to accomplish this have been shown to reliably prevent the recognition of particular individuals (Bischoff-Grethe et al., in press). Here, we have additionally shown that these methods do not significantly impact typical calculations of anatomical measures such as intracranial volume and whole-brain volume.

The specific anatomical measures included here, eTIV and nWBV, are illustrative of approaches commonly used to analyze anatomical characteristics of the brain in MRI images, particularly in relation to aging. Unsurprisingly, our findings are in agreement with those described in previous studies using portions of these data before defacing (Fotenos et al., 2005; Buckner et al., 2004). In particular, eTIV was shown to differ little with age and dementia status. Because the atlas-based methods used to generate eTIV are entirely automated, eTIV is an attractive alternative to laborious manual TIV measures for correcting for head size in studies of aging and dementia. nWBV, on the other hand, was shown to decline across the adult life span with acceleration in advanced aging, consistent with findings from a broad range of studies (see DeCarli et al., 2005; Fotenos et al., 2005; Sowell, Thompson, & Toga, 2004; Durston, 2003; Blatter et al., 1995, for reviews). Marked volume loss was observed in AD.

This distribution also includes data from 20 individuals who were scanned on two occasions separated by a short interval. Because little real change in anatomical structure is likely to have occurred between the two acquisitions, these images are useful for estimating the reliability of analytic methods. The measures of eTIV and nWBV described here provide a reference point for the amount of error seen with established approaches. However, because these scans were all obtained from young healthy individuals, reliability may be overestimated relative to a sample of older subjects with dementia who are more prone to movement and other artifacts.

Although other publicly available neuroimaging data sets are available, most notably those provided by the Alzheimer's Disease Neuroimaging Initiative (ADNI), the present data set contributes complimentary features. First, ADNI targets mild cognitive impairment and AD and, by design, includes a limited number of older adults without dementia and no individuals before middle age. The present data set targets the full adult life span and, therefore, allows exploration of aging in addition to effects of AD. Second, ADNI is a multicenter study that will be extremely valuable for developing methods that can pool across sites. There will not, however, be a large quantity of matched data sets from the same scanner/sequence type. The present data includes more than 400 subjects with data collected on the identical platform with identical sequences. Finally, in the present data set, multiple acquisitions were acquired for each subject within session to allow substantial signal averaging. This is not typically done, and this choice was made to optimize our data for exploration of automated

computational analyses, including measures of cortical thickness and fine demarcation of subcortical regions. The result is 416 scanning sessions, each with high-contrast imaging data that are amenable to a wide range of computational analyses.

A number of additional data sets are planned as part of the OASIS project. These will include longitudinal acquisitions of individuals with and without dementia, acquisitions from subjects obtained on multiple different scanners, functional MRI of cognition, and resting-state functional MRI for noise analysis and analysis of spontaneous low-frequency signals. Following the principles established with the initial release, these sets will be carefully prepared, vetted, and described.

Acknowledgments

REFERENCES

Berg, L., Hughes, C. P., Coben, L. A., Danziger, W. L., Martin, R. L., & Knesevich, J. (1982). Mild senile dementia of Alzheimer type: Research diagnostic criteria, recruitment, and description of a study population. *Journal of Neurology, Neurosurgery and Psychiatry, 45,* 962–968.

Berg, L., McKeel, D. W., Jr., Miller, J. P., Storandt, M., Rubin, E. H., Morris, J. C., et al. (1998). Clinicopathologic studies in cognitively healthy aging and Alzheimer's disease: Relation of histologic markers to dementia severity, age, sex, and apolipoprotein E genotype. *Archives of Neurology, 55,* 326–335.

Bischoff-Grethe, A., Ozyurt, I. B., Busa, E., Quinn, B. T., Fennema-Notestine, C., Clark, C. P., et al. (in press). A technique for the deidentification of structural brain MR images. *Human Brain Mapping.*

Blatter, D. D., Bigler, E. D., Gale, S. D., Johnson, S. C., Anderson, C. V., Burnett, B. M., et al. (1995). Quantitative volumetric analysis of brain MR: Normative database spanning 5 decades of life. *American Journal of Neuroradiology, 16,* 241–251.

Buckner, R. L., Head, D., Parker, J., Fotenos, A. F., Marcus, D., Morris, J. C., et al. (2004). A unified approach for morphometric and functional data analysis in young, old, and demented adults using automated atlas-based head size normalization: Reliability and validation against manual measurement of total intracranial volume. *Neuroimage, 23,* 724–738.

Buckner, R. L., Quinn, B. T., Salat, D. H., Head, D., Snyder, A. Z., Busa, E., et al. (in press). Evidence for distinct effects of aging and Alzheimer's disease on the hippocampus. *Journal of Neuroscience.*

Buckner, R. L., Snyder, A. Z., Shannon, B. J., LaRossa, G., Sachs, R., Fotenos, A. F., et al. (2005). Molecular, structural, and functional characterization of Alzheimer's disease: Evidence for a relationship between default activity, amyloid, and memory. *Journal of Neuroscience, 25,* 7709–7717.

Burns, J. M., Church, J. A., Johnson, D. K., Xiong, C., Marcus, D., Fotenos, A. F., et al. (2005). White matter lesions are prevalent but differentially related with cognition in aging and early Alzheimer disease. *Archives of Neurology, 62,* 1870–1876.

Coffey, C. E., Lucke, J. F., Saxton, J. A., Ratcliff, G., Unitas, L. J., Billig, B., et al. (1998). Sex differences in brain aging: A quantitative magnetic resonance imaging study. *Archives of Neurology, 55,* 169–179.

Coffey, C. E., Saxton, J. A., Ratcliff, G., Bryan, R. N., & Lucke, J. F. (1999). Relation of education to brain size in normal aging: Implications for the reserve hypothesis. *Neurology, 53,* 189–196.

Csernansky, J. G., Wang, L., Joshi, S. C., Ratnanather, J. T., & Miller, M. I. (2004). Computational anatomy and neuropsychiatric disease: Probabilistic assessment of variation and statistical inference of group difference, hemispheric asymmetry, and time-dependent change. *Neuroimage, 23 (Suppl. 1),* S56–S68.

DeCarli, C., Massaro, J., Harvey, D., Hald, J., Tullberg, M., Au, R., et al. (2005). Measures of brain morphology and infarction in the Framingham Heart Study: Establishing what is normal. *Neurobiology of Aging, 26,* 491–510.

Desikan, R. S., Segonne, F., Fischl, B., Quinn, B. T., Dickerson, B. C., Blacker, D., et al. (2006). An automated labeling system for subdividing the human cerebral cortex on MRI scans into gyral based regions of interest. *Neuroimage, 31,* 968–980.

Durston, S. (2003). A review of the biological bases of ADHD: What have we learned from imaging studies? *Mental Retardation and Developmental Disabilities Research Reviews, 9,* 184–195.

Fischl, B., Salat, D. H., Busa, E., Albert, M., Dieterich, M., Haselgrove, C., et al. (2002). Whole brain segmentation: Automated labeling of neuroanatomical structures in the human brain. *Neuron, 33,* 341–355.

Folstein, M. F., Folstein, S. E., & McHugh, P. R. (1975). ''Mini-Mental State.'' A practical method for grading the cognitive state of patients for the clinician. *Journal of Psychiatric Research, 12,* 189–198.

Fotenos, A. F., Mintun, M. A., Snyder, A. Z., Morris, J. C., & Buckner, R. L. (in press). Brain volume decline in aging: Evidence for a relationship between socioeconomic status, preclinical AD, and reserve. *Journal of Neuroscience.*

Fotenos, A. F., Snyder, A. Z., Girton, L. E., Morris, J. C., & Buckner, R. L. (2005). Normative estimates of cross-sectional and longitudinal brain volume decline in aging and AD. *Neurology, 64,* 1032–1039.

Head, D., Snyder, A. Z., Girton, L. E., Morris, J. C., & Buckner, R. L. (2005). Frontal–hippocampal double dissociation between normal aging and Alzheimer's disease. *Cerebral Cortex, 15,* 732–739.

Hollingshead, A. (1957). *Two factor index of social position.* New Haven, CT: Yale University Press.

Jack, C. R., Jr., Petersen, R. C., O'Brien, P. C., & Tangalos, E. G. (1992). MR-based hippocampal volumetry in the diagnosis of Alzheimer's disease. *Neurology, 42,* 183–188.

Jack, C. R., Jr., Petersen, R. C., Xu, Y. C., Waring, S. C., O'Brien, P. C., Tangalos, E. G., et al. (1997). Medial temporal atrophy on MRI in normal aging and very mild Alzheimer's disease. *Neurology, 49,* 786–794.

Killiany, R. J., Moss, M. B., Albert, M. S., Sandor, T., Tieman, J., & Jolesz, F. (1993). Temporal lobe regions on magnetic resonance imaging identify patients with early Alzheimer's disease. *Archives of Neurology, 50,* 949–954.

Koga, H., Yuzuriha, T., Yao, H., Endo, K., Hiejima, S., Takashima, Y., et al. (2002). Quantitative MRI findings and cognitive impairment among community dwelling elderly subjects. *Journal of Neurology, Neurosurgery and Psychiatry, 72,* 737–741.

Marcus, D. S., Olsen, T., Ramaratnam, M., & Buckner, R. L. (2007). The extensible neuroimaging archive toolkit (XNAT): An informatics platform for managing, exploring, and sharing neuroimaging data. *Neuroinformatics, 5,* 11–34.

McKhann, G., Drachman, D., Folstein, M., Katzman, R., Price, D., & Stadlan, E. M. (1984). Clinical diagnosis of Alzheimer's disease: Report of the NINCDS-ADRDA Work Group under the auspices of Department of Health and Human Services Task Force on Alzheimer's Disease. *Neurology, 34,* 939–944.

Morris, J. C. (1993). The Clinical Dementia Rating (CDR): Current version and scoring rules. *Neurology, 43,* 2412–2414.

Morris, J. C., Storandt, M., Miller, J. P., McKeel, D. W., Price, J. L., Rubin, E. H., et al. (2001). Mild cognitive impairment represents early-stage Alzheimer disease. *Archives of Neurology, 58,* 397–405.

Mugler, J. P., III, & Brookeman, J. R. (1990). Three-dimensional magnetization-prepared rapid gradient-echo imaging (3D MP RAGE). *Magnetic Resonance in Medicine, 15,* 152–157.

Raz, N., Gunning, F. M., Head, D., Dupuis, J. H., McQuain, J., Briggs, S. D., et al. (1997). Selective aging of the human cerebral cortex observed in vivo: Differential vulnerability of the prefrontal gray matter. *Cerebral Cortex, 7,* 268–282.

Raz, N., Rodrigue, K. M., & Acker, J. D. (2003). Hypertension and the brain: Vulnerability of the prefrontal regions and executive functions. *Behavioral Neuroscience, 117,* 1169–1180.

Raz, N., Williamson, A., Gunning-Dixon, F., Head, D., & Acker, J. D. (2000). Neuroanatomical and cognitive correlates of adult age differences in acquisition of a perceptual–motor skill. *Microscopy Research and Techniques, 51,* 85–93.

Salat, D. H., Buckner, R. L., Snyder, A. Z., Greve, D. N., Desikan, R. S., Busa, E., et al. (2004). Thinning of the cerebral cortex in aging. *Cerebral Cortex, 14,* 721–730.

Scheltens, P., Leys, D., Barkhof, F., Huglo, D., Weinstein, H. C., Vermersch, P., et al. (1992). Atrophy of medial temporal lobes on MRI in ''probable'' Alzheimer's disease and normal ageing: Diagnostic value and neuropsychological correlates. *Journal of Neurology, Neurosurgery and Psychiatry, 55,* 967–972.

Snyder, A. Z. (1996). Difference image vs ratio image error function forms in PET–PET realignment. In D. Bailey & T. Jones (Eds.), *Quantification of brain function using PET* (pp. 131–137). San Diego, CA: Academic Press.

Sowell, E. R., Thompson, P. M., Leonard, C. M., Welcome, S. E., Kan, E., & Toga, A. W. (2004). Longitudinal mapping of cortical thickness and brain growth in normal children. *Journal of Neuroscience, 24,* 8223–8231.

Sowell, E. R., Thompson, P. M., & Toga, A. W. (2004). Mapping changes in the human cortex throughout the span of life. *Neuroscientist, 10,* 372–392.

Storandt, M., Grant, E. A., Miller, J. P., & Morris, J. C. (2006). Longitudinal course and neuropathologic outcomes in original vs revised MCI and in pre-MCI. *Neurology, 67,* 467–473.

Styner, M., Brechbuhler, C., Szekely, G., & Gerig, G. (2000). Parametric estimate of intensity inhomogeneities applied to MRI. *IEEE Transactions on Medical Imaging, 19,* 153–165.

Talairach, J., & Tournoux, P. (1988). *Co-planar stereotaxic atlas of the human brain: An approach to medical cerebral imaging.* New York: Thieme.

Zhang, Y., Brady, M., & Smith, S. (2001). Segmentation of brain MR images through a hidden Markov random field model and the expectation–maximization algorithm. *IEEE Transactions on Medical Imaging, 20,* 45–57.